This is the peer reviewed version of the following article: *Sergio F. Castillo Pacheco, Maria Jesus Moran, José I. Santos, Luca Salassa, Fernando López-Gallego. Chemoenzymatic Oxidation of Diols Catalyzed by Co-Immobilized Flavins and Dehydrogenases. ChemCatChem 2023*, which has been published in final form at https://doi.org/10.1002/cctc.202300140.

This article may be used for non-commercial purposes in accordance with Wiley Terms and Conditions for Use of Self-Archived Versions.

Chemoenzymatic Oxidation of Diols Catalyzed by Co-Immobilized Flavins and Dehydrogenases

Sergio F. Castillo Pacheco,[a,b] Maria Jesus Moran,*[b] José I. Santos,[c] Luca Salassa[b,d,e] and Fernando López-Gallego*[a,e]

[a] M.Sc S. F. Castillo Pacheco, Prof. F. López-Gallego
Heterogeneous Biocatalysis Laboratory, Center for Cooperative Research in Biomaterials (CIC biomaGUNE), Basque Research and Technology Alliance (BRTA), Paseo de Miramon 182, 20014, Donostia, Spain
E-mail: flopez@cicbiomagune.es; https://flg802.wixsite.com/flopezgallego/lopez-gallego

[b] M.Sc S. F. Castillo Pacheco, Dr. M.J. Moran, Prof. L. Salassa
Donostia International Physics Center,
Paseo Manuel de Lardizabal 4, 20018 Donostia, Spain
E-mail: mariajesus.moran@dipc.org

[c] Dr. J. I. Santos
SGIker-UPV/EHU, "Joxe Mari Korta" Zentroa,
Tolosa Hiribidea 72, 20018 Donostia, Euskadi, Spain

[d] Prof. L. Salassa
Polimero eta Material Aurreratuak: Fisika, Kimika eta Teknologia, Kimika Fakultatea, Euskal Herriko Unibertsitatea UPV/EHU,
Paseo Manuel de Lardizabal 3, 20018 Donostia, Spain

[e] Prof. L. Salassa, Prof. F. López-Gallego
Ikerbasque, Basque Foundation for Science,
48011 Bilbao, Spain

Abstract: Enzyme driven oxidations catalyzed by alcohol dehydrogenases rely on the *in situ* NAD(P)$^+$ regeneration. A wide variety of chemoenzymatic and fully enzymatic methods have been reported over the last 30 years to integrate the cofactor regeneration in biocatalytic oxidations. However, the majority of examples are limited to homogeneous systems where the reuse of both enzymes and chemical catalysts are challenging. In this work, we co-immobilize an alcohol dehydrogenase from *Bacillus stearothermophilus* with a flavin derivative (**FMN**), which performs as an organocatalyst that oxidizes NADH back to NAD$^+$. This latter oxidized cofactor is sequentially utilized by the dehydrogenase to oxidize 1,ω-diols. Remarkably, the immobilization chemistry of **FMN** determines its efficiency to oxidize NADH and, unlike in its free state, the immobilized **FMN** can recycle NAD$^+$ in dark. This is possible because the support where both enzyme and **FMN** are immobilized also captures NADH, making the electron transfer from the substrates to the cofactors more efficient. This work illustrates how the co-immobilization and confinement of bio and chemical catalysts on solid materials (heterogeneous phase) enable chemoenzymatic cascades that are precluded in solution (homogeneous phase).

Introduction

Oxidative reactions are one of the pillars that sustain the organic synthesis toolbox, because ketones, aldehydes, lactones and acids are massively used in the chemical industry for the manufacturing of cosmetics, agrochemicals, and pharmaceuticals. Unfortunately, most of the oxidative processes carried out at large scale are typically performed with stoichiometric reagents that produce hazardous waste and use solvents poorly compatible with the environment. [1] For those advanced oxidative processes that employ metals (i.e. Pt and Pd) as catalysts to improve the process sustainability, the global industry faces the risk of economic and geopolitical shortages for minerals containing precious metals. [2] Herein, biocatalysis emerges as a transformative technology that makes chemical processes more sustainable and less dependent on global trading.[3] However, when oxidation reactions are catalyzed by dehydrogenases, an efficient system for regenerating *in situ* the redox nicotinamide cofactor (NAD$^+$) is needed to make the enzymatic process sustainable and cost-efficient. For oxidations, NAD$^+$-recycling systems majorly rely on NADH oxidase (NOX), a flavin-dependent oxidase that converts NADH to NAD$^+$. [4],[5] This enzyme is very attractive because it utilizes molecular oxygen as ultimate electron acceptor, which favors the reaction thermodynamics and produces innocuous byproducts (oxygen and water). As alternative to the NOX-driven NAD$^+$ recycling, laccase-mediated systems (LMS) have also been exploited. LMS are chemoenzymatic systems where an electron shuttle (i.e. acetosyringone) is first oxidized by the laccase at the expense of molecular oxygen. Then, the mediator is reduced back to its initial state by NADH, yielding NAD$^+$ in an uncatalyzed reaction. Also flavin oxidoreductases and free flavins as mediators have been using in biocatalytic oxidations to regenerate the pool of NAD$^+$.[5]

Inspired by the pioneering work of Jones and Taylor,[6] Rauch et al. exploited free flavin as photocatalysts to recycle *in situ* the NAD$^+$ pool required by an alcohol dehydrogenase from horse liver that oxidizes 1,ω-diols to δ-

valerolactone.[7] In the absence of light, this reaction occurred negligibly, making the system impractical for manufacturing purposes. Recently, our groups demonstrated that NADH could be effectively oxidized in the dark when a platinum coordination compound is used as the ultimate electron acceptor by co-immobilization of **FMN** and NADH on porous materials, such as agarose (AG) microbeads, through electrostatic interactions. [8],[9] This system mimics the cofactor organization of most NADH oxidases (NOX) as both **FMN** and NADH intimately co-localize across the structure of the porous chassis in which they are confined. [10] Thus, the chances for electron transfer between the two cofactors increase, although the flavin is not photoexcited. Following a similar approach, Chen *et al.* co-immobilized **FMN** and NADH on zeolitic imidazolate frameworks encapsulated with polyethylenimine.[11] This material was then coupled with a free alcohol dehydrogenase for integrating ethanol oxidation with *in situ* NAD^+ recycling in the dark. However, this design did not afford enzyme recycling together with the heterogenous flavin.

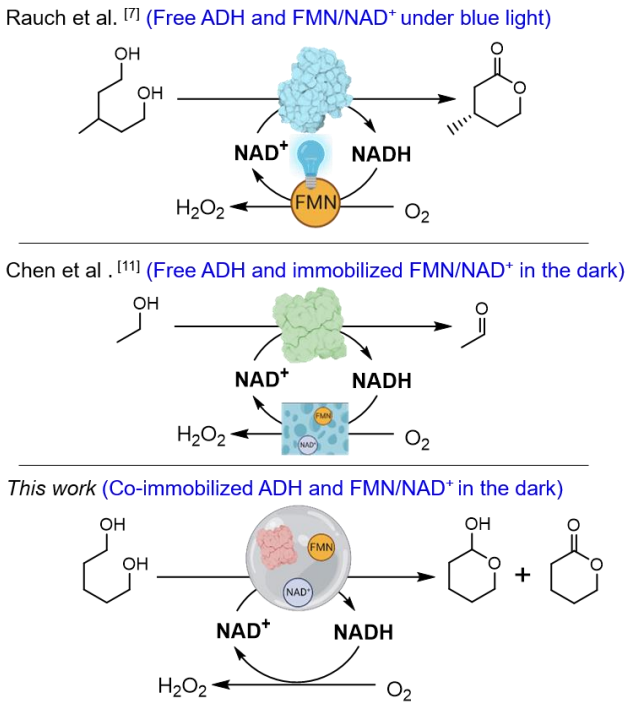

Scheme 1. Different approaches for the chemoenzymatic oxidation of alcohols using flavins as organocatalysts for *in situ* NAD^+ regeneration. ADH: Alcohol dehydrogenase.

In this work, we make one step further compared to the systems already described by designing a fully heterogeneous (organo)biocatalyst, where enzymes and cofactors are immobilized on the same porous support. In this architecture, the cofactor regeneration driven by an artificial NOX (flavin and NADH co-immobilized) shall occur within the pores and in the surroundings of the alcohol dehydrogenase. Hence, we propose an innovative heterogeneous chemoenzymatic system where an enzyme catalyzes the substrate oxidation, and an organocatalyst (which can additionally act as photocatalyst) performs the cofactor recycling. To build up this hybrid (chemo)biocatalyst, we first studied different immobilization chemistries for selected flavins to find the most efficient heterogeneous organocatalysts for the NADH oxidation, under either light-irradiated (456 nm) or dark conditions. Then, we co-immobilized the most active flavins with a model alcohol dehydrogenase from *Bacillus stearothermophilus* and challenged these heterogeneous chemoenzymatic systems to the selective oxidation of 1,ω-diols as model reaction. Results showed that the alcohol dehydrogenase was inactivated by light irradiation in the presence of the flavin, however, this catalytic pair worked when both enzyme and flavin (**FMN** in this case) were co-immobilized on agarose porous microbeads through electrostatic interactions and operated in the dark.

Results and Discussion

We initially evaluated how the immobilization chemistry affects the NADH oxidase activity of the flavins bound to AG supports. In the first instance, we immobilized **FMN** onto AG beads functionalized with diethyl aminoethyl groups (AG-DEAE) through electrostatic interactions, as previously reported.[8] So, we obtained catalysts, dubbed

as **FMN**@AG-DEAE, that were loaded with 0.69–5.79 μmol g^{-1} of flavin (entries 1-3). In parallel, we synthesized an aminated flavin (**Rf-NH₂**) by N3 functionalization of riboflavin with a Br-alkyl amine (see Supporting Information, Figure S1-S6) and explored its covalent attachment on porous AG beads, bearing epoxide (AG-E, Table 1, entries 4-6, Figure S7) or aldehyde groups (AG-G, Table 1, entries 7-10). Epoxides/aldehydes displayed at the support surface easily undergo nucleophilic addition of primary amines under alkaline conditions.[12] Flavin immobilization yield and loading were assessed by UV-Vis spectroscopy (see Supporting Information, Figure S8). As depicted in Table 1, 3 mM of **Rf-NH₂** resulted to be the optimal offered concentration to achieve the highest immobilization yields and loads (Table 1, entries 6 and 10).

Table 1. Immobilization parameters for the binding of different flavins to selected supports.

Entry	Support	Flavin	Offered conc. (mM)[a]	Yield (%)	Flavin Loading (μmol g^{-1})
1	AG-DEAE	**FMN**	0.15	46	0.7
2	AG-DEAE	**FMN**	0.5	56	2.8
3	AG-DEAE	**FMN**	1	58	5.8
4	AG-E	**Rf-NH₂**	0.5	62	3.1
5	AG-E	**Rf-NH₂**	1	63	6.3
6	AG-E	**Rf-NH₂**	3	68	2.1
7	AG-G	**Rf-NH₂**	0.15	28	0.4
8	AG-G	**Rf-NH₂**	0.5	48	2.4
9	AG-G	**Rf-NH₂**	1	31	3.1
10	AG-G	**Rf-NH₂**	3	48	14.4

[a] Offered flavin concentration is determined by UV-Vis spectroscopy.

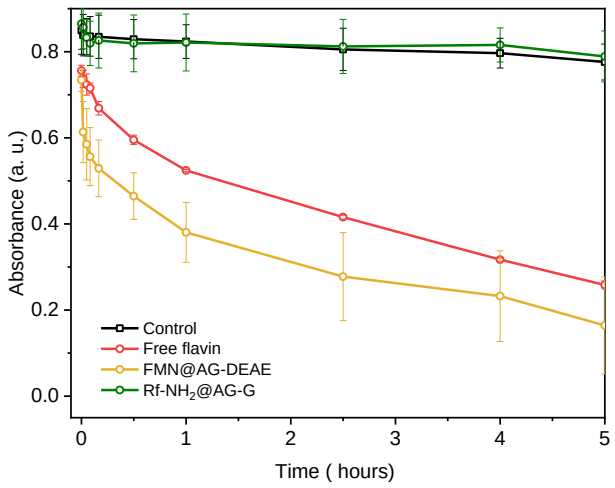

Figure 1. Time courses for the NADH oxidation catalyzed by free and immobilized flavins in darkness. The reactions were performed at the NADH:flavin molar ratios of 10:1 fixing NADH concentration at 0.4 mM under stirring conditions (25 ºC). The black line is the NADH control without flavin.

AG-G reached loadings of up to 14.43 μmol of **Rf-NH₂** per wet g of AG, affording an immobilized flavin system dubbed as **Rf-NH₂**@AG-G (Table 1, entry 10). The presence of **Rf-NH₂** onto AG beads was confirmed by solid-state CP-MAS ^{13}C NMR (Figure S9) and epifluorescence microscopy (Figure S10). Once **FMN** and **Rf-NH₂** were successfully immobilized on agarose beads, we tested how the two heterogeneous catalysts, **FMN**@AG-DEAE and **Rf-NH₂**@AG-G, performed in the NADH to NAD^+ oxidation. Figure 1 shows the time courses of the NADH

oxidation in the dark under stirring conditions. As a benchmark system, we compared the immobilized flavins with their soluble counterpart. Under these conditions, the NADH oxidation initial rate of both free **Rf-NH$_2$** and **FMN** (Figure 1, red line) was 1.7 times lower than to that observed for **FMN**@AG-DEAE (Figure 1, yellow line), yet 14-fold higher than that exhibited by **Rf-NH$_2$**@AG-G (Figure 1, green line). A similar trend was observed when the organocatalysts worked under light (Figure S11), however the reaction was completed in minutes instead of hours, indicating that light accelerates the reaction, even at the solid phase, by a 40-fold factor. Only under this conditions **Rf-NH$_2$**@AG-G was able to fully oxidize NADH (Figure S11B). These time courses demonstrate that **FMN**, if immobilized, must be confined with its electron donor (NADH) to boost its artificial NOX activity. Furthermore, we demonstrated that the supported flavin, as well as its free counterpart, were significantly more active when working under light irradiation, in agreement with previous results of our groups.[8-9, 13]

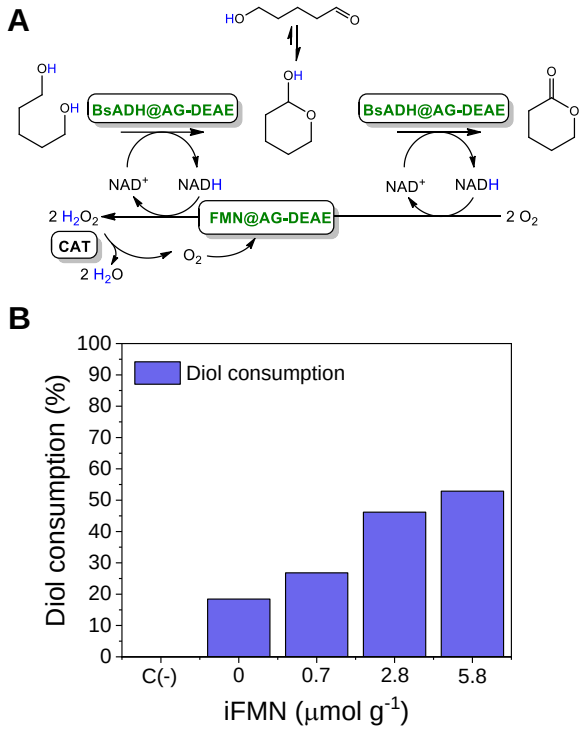

Figure 2. (**A**) Selective oxidation of 1,5–pentanodiol to 5-hydroxypentanal, in equilibrium with 2-hydroxytetrahydropyran which can be further oxidized to δ-valerolactone, integrating a NAD$^+$ recycling systems. This biotransformation is catalyzed by an heterogeneous (organo)enzymatic catalyst (BsADH/**FMN**@AG-DEAE) aided by a free catalase (CAT), which in situ removes H_2O_2 resulted from the aerobic reoxidation of the flavin (**B**). Diol conversion at different loadings of immobilized **FMN** (iFMN). 10 mM of 1,5-pentanodiol, 2 mM of NAD$^+$ and 50 U of catalase from bovine liver (CAT). The negative control (C(-)) is the reaction performed without the addition of ADH (**FMN** and NAD$^+$ in solution). Reaction conditions: volume of 200 µl, 30ºC, pH 7 and stirring of 250 rpm.

Next, we assessed the capacity of the flavin to replenish the pool of NAD$^+$ in a dehydrogenase driven oxidation. As model reaction, we selected the oxidation of 1,5-pentanodiol to 5-hydropentanal. The latter is in equilibrium with lactol (2-hydroxytetrahydropyran) upon the spontaneous formation of the intramolecular hemiacetal. This oxidation is catalyzed by the alcohol dehydrogenase from *Bacillus stearothermophilus* (BsADH), which can also perform the subsequent oxidation of lactol to ultimately yield δ-valerolactone (Figure 2A).[4, 14] When we performed the reaction under light, we surprisingly detected no product (neither lactol nor lactone). To investigate the photochemical robustness of BsADH, we incubated the free enzyme with free **FMN** in the same reaction media, yet without substrate. We observed the complete inactivation of the free BsADH upon exposure to blue light in presence of the flavin, while the same enzyme retained more than 70% of its initial activity under the same conditions without the flavin (Figure S12). This photoinactivation may rely on the production of single oxygen and hydrogen peroxide upon the flavin regeneration under aerobic conditions. Additionally, direct photooxidation of amino acid residues by the flavin triplet excited state could be another factor responsible for shutting down the enzyme activity.[15]
In an attempt to avoid the deleterious effect of the light on free BsADH when a soluble flavin was present, we co-immobilized the enzyme with either **FMN** or **Rf-NH$_2$** onto AG-DEAE or AG-G, respectively. In the first case, anchoring of **FMN** and the enzyme was achieved through electrostatic interactions at pH 7. In the latter, **Rf-NH$_2$** and BsADH were attached covalently under

Table 2. Parameters for the co-immobilization of BsADH and flavins onto different AG supports.

Entry	Support	Flavin	Offered flavin concentration (mM)	ADH Loading (mg g^{-1})	Immob. efficiency (η)
1	AG-G	**Rf-NH_2**	0.15	1	0.1
2	AG-DEAE	**FMN**	0.15	1	0.1
3	AG-DEAE	**FMN**	0.5	1	0.1
4	AG-DEAE	**FMN**	1	1	0.1

[a] Offered flavin concentration was determined by UV-Vis spectroscopy.

alkaline conditions (pH 10) exploiting their available primary amino groups, followed by an imine reduction step with $NaBH_4$ to obtain a more stable attachment (secondary amine) which irreversibly anchored the two components to the support. Table 2 shows the loadings and immobilization effectiveness (□) for both flavin derivatives and alcohol dehydrogenases on the different AG supports. In all cases, BsADH was quantitatively immobilized on AG-G and AG-DEAE achieving 1 mg g^{-1} loading, and recovered roughly 10% of its initial activity upon immobilization (η of 0.1). Remarkably, AG-supported **FMN** or **Rf-NH_2** and BsADH kept 100% of their activity after 3-day storage at 4º C. When we performed oxidation tests with these heterogeneous (organo)biocatalysts under light irradiation, no product formation was detected in the reaction media, suggesting that the co-immobilization of the flavin and the enzyme failed to avoid the photoinactivation of BsADH (Figure S12). In contrast, we detected lactol and lactone using BsAHD/**FMN**@AG-DEAE with NAD^+ in the dark, suggesting that the immobilized **FMN** was working as NADH oxidase coupled to BsADH. This was possible due to the electrostatic absorption of NAD^+ onto the AG-DEAE surface, where colocalization with the immobilized **FMN** and BsADH facilitated the electron transfer from the enzymatically produced NADH to the flavin. To confirm that the co-immobilization of the flavin and the dehydrogenase is the driver of the *in situ* regeneration of NAD^+ in the absence of light, we performed the reaction in the dark using free **FMN** and BsADH. In agreement with Rauch *et al.*, [7] we observed no diol oxidation using substoichiometric amounts of free flavin with respect to NADH. Similar results were observed for the oxidation of diols using a dehydrogenase from horse liver and **FMN**.[7] Therefore, NADH oxidation can only be catalyzed by **FMN** if the two redox cofactors co-localize in a confined space like the porous surface of AG-DEAE. Encouraged by these findings we challenged the BsADH/**FMN**@AG-DEAE system in the oxidation of 1,5-pentanodiol in presence of soluble bovine liver catalase (CAT). This latter enzyme was needed to remove H_2O_2 formed *in situ* by the spontaneous aerobic reoxidation of the reduce flavin (**FMN**H_2) upon the NADH oxidation.[16] Figure 2B shows that this heterogenous (organo)catalyst could oxidize the diol although with a very low conversion (30%), yet still higher than the conversion achieved without **FMN**, indicating that BsADH was active in presence of **FMN**. With low **FMN** loadings (0.7 µmol g^{-1}), the turnover of NAD^+ was only 1.5, but it proved that **FMN** recycled the pool of NAD^+ upon its dehydrogenase-driven reduction in the dark. Under these conditions, 1 mM of NAD^+ was recycled by only 0.1 mM of **FMN** bound to the support, which means a total turnover number (TTN) of the flavin equal to 10. The diol conversion increased along with the loading of **FMN** on the AG-DEAE support. At **FMN** loadings as high as 5.8 µg g^{-1}, 50% of the diol was converted. As the loading increased the TTN of flavin lowered from 10 to 2.8, however the TTN of the BsADH did improve from 2.6 x 10^3 to 4 x 10^3.

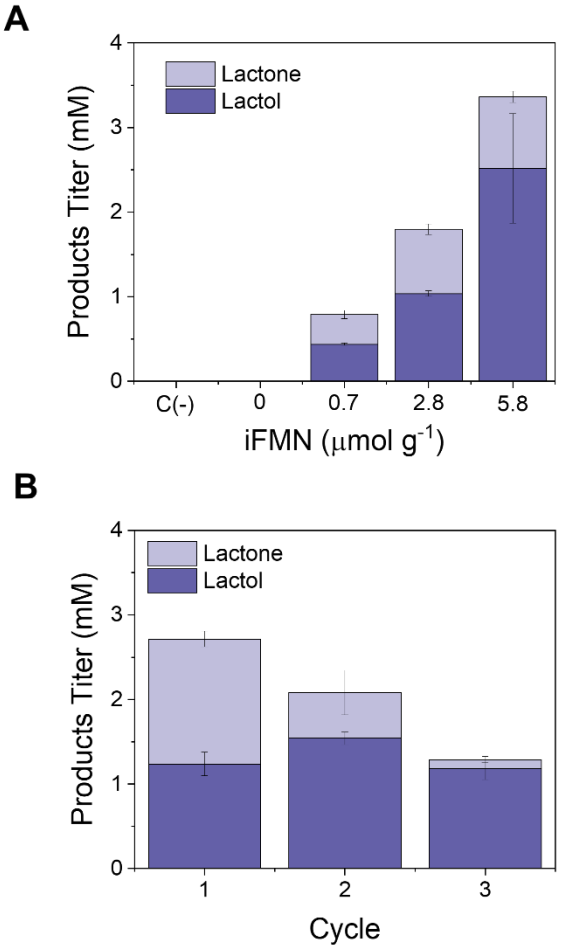

Figure 3. **(A)** Product profile (lactol: 2-hydroxytetrahydropyran, and lactone: δ-valerolactone) at different loadings of immobilized **FMN** (iFMN). 10 mM of 1,5-pentanodiol, 2 mM of NAD^+ and 50 U of catalase from bovine liver (CAT). The negative control (C(-)) is the reaction performed without the addition of BsADH (**FMN**, substrate and NAD^+ in solution). Reaction conditions: volume of 200 µl, 30ºC, pH 7 and stirring at 250 rpm and 30-42 µg of solid catalyst. **(B)** Consecutive batch cycles using the same BsADH/**FMN**@AG-DEAE (organo)enzymatic heterogeneous biocatalysts loaded with 5.3 µmol g^{-1} **FMN**. Reaction conditions were the same as described in **A**.

conversion) Finally, we studied the effect of the **FMN** loading (iFMN) in the product outcome of this heterogeneous (organo)biocatalyst and the reusability of the most productive one along consecutive batch reaction cycles. Figure 3A shows the reaction outcome was maintained at the different flavin loadings, resulting in a lactol:lactone molar ratio of 2:1, which confirmed that the lactol oxidation is the rate limiting step of this sequential oxidation.[14] At the highest FMN load, the heterogeneous (organo)biocatalysts oxidized 5 mM diol (50%into 3 mM of lactol and 1 mM of lactone. The mass balance of this reaction did not perfectly close, likely due to the spontaneous hydrolysis of the lactone to the corresponding 5-hydroxy pentanoic acid and the undetected 5-hydroxypentanal, as previously observed in a similar biotransformation.[7] According to this product outcome and without considering the possible spontaneous hydrolysis of the lactone, 6 mM of NAD^+ (5 mM from diol oxidation and 1 mM extra from lactol to lactone oxidation) were reduced to NADH, resulting in a NAD^+ turnover of 3 since the reaction was initially triggered with 2 mM NAD^+. After the second cycle the product yield decreased dramatically and in the third cycle (Figure 3B), indicating a severe operation inactivation of the heterogeneous (organo)biocatalyst under the working conditions. Similar results were achieved co-immobilizing the catalase with **FMN** and BsADH on AG-DEAE (Figure S13), demonstrating that the completed system can be re-used. In order to explain the causes that drive the inactivation of the heterogeneous (organo)biocatalyst under operational conditions, we studied the lixiviation of **FMN** and BsADH. To this aim, we first analyzed the **FMN** lixiviation by measuring the **FMN** concentration in the reaction crudes upon each cycle (Figure S14). We found out that the electrostatically bound flavin leaches into the reaction crude, diminishing the available organocatalyst load for the following cycles. To overcome this issue, we added fresh FMN upon each cycle, achieving a similar product titer after two consecutive cycles (Figure S15), but a significantly lower titer of mainly lactol after the third cycle. Therefore, **FMN** lixiviation is not the only cause that explains the operational inactivation of the system. To investigate whether the BsADH was inactive after the third operational cycle we measured its residual activity in the immobilized system by a colorimetric assay (Figure S16). This assay evidenced the practical inactivation of the

enzyme upon its discontinuous use in three operational cycles. SDS-PAGE analysis confirmed that the activity loss upon use is due to the dramatic lixiviation of BsADH after the third operational cycle (Figure S17).

Conclusions

In this work we have assembled for the first time a supported (organo)enzymatic system for the selective oxidation of alcohols which is independent of an enzymatic regeneration system. Herein, the cofactor recycling is catalyzed by protein-unbound flavins without demanding light for their photoexciation. This has been possible through the co-immobilization of alcohol dehydrogenase and a free flavin on porous surfaces through electrostatic interactions. The porous surface acted as a chassis for both the enzyme and the organocatalyst (the flavin), but also as an absorbent that captured and concentrated NADH in the surroundings of **FMN** to increase the efficiency of electron transfer from the nicotinamide cofactor to the isoalloxazine ring of the flavin. This spatial organization made possible the NAD^+ recycling demanded by the dehydrogenase for the alcohol oxidation in dark conditions, otherwise impossible using free cofactors and enzymes. Unfortunately, this reaction could not be intensified by light irradiation due to the dehydrogenase inactivation driven by the photoexcited flavin. However, we envision that it will inspire other spatial organizations capable of avoiding such catalyst incompatibility. Finally, the reusability of the system was proven although it requires further optimization to prevent the lixiviation of both the organo and biocatalysts from the solid support. In our opinion, the study herein presented contributes to expand the number of examples where chemo and biocatalysts are combined to fabricate hybrid heterogenous catalysts with advanced properties unreachable by chemical catalysts and enzymes by their own.

Experimental Section

Materials

All reagents used were commercial grade chemicals from freshly opened containers. Mili-Q water was purified with a Milipore Gradient A10 apparatus. Silica gel (0.035-0.070 mm, 60 Å) was used for flash chromatography and Merck 60 F254 foils were used for thin layer chromatography. Riboflavin 5'-monophosphate sodium salt hydrate (**FMN**), (-)-riboflavin, dimethoxypropane, cesium carbonate (Cs_2CO_3), β-nicotinamide adenine dinucleotide reduced disodium salt hydrate (NADH), tris(hydroxymethyl)aminomethane (Tris) were purchased by Merk. 3-bromopropylamine hydrobromide and p-toluenesulfolyl acid monohydrate (p-TsOH) were procured from Fisher. Di-tert-butyl dicarbonate (Boc-anhydride) was purchased from Alfa Aesar. Trifluoroacetic acid (99%, extra pure) was obtained from ACROS Organics™. Diethylaminoethyl agarose microbeads (AG-DEAE) were acquired from GE Healthcare.

Synthesis of the 3-(7,8-dimethyl-2,4-dioxo-10-((2R,3R,4S)-2,3,4,5-tetrahydroxypentyl)-4,10-dihydrobenzo[g]pteridin-3(2H)-yl)propan-1-aminium (III) (Rf-NH_2)

Rf-NH_2 was synthesized and characterized as previously described by Mazzei et al.[17] Reaction scheme and all the characterization are reported in the Supporting Information (Figures S1-S6).

Intermediate 2: Riboflavin (**1**) (3.76 g, 10 mmol) was suspended in 50 mL of DMF:Acetone (1:1) (50 mL). Dimethoxypropane (17g, 163 mmol) and p-TsOH·H_2O (1.9 g, 10 mmol) were added and the mixture was left stirring at room temperature for 4 days. The solvent was then evaporated in the rotavapor under reduced pressure. The remaining reaction crude was extracted in CH_2Cl_2:LiCl (aq.10%, 50 mL x 3) and dried with $MgSO_4$. 2.5 g of yellow solid was obtained after removing the solvent in the rotavapor. Yield: 55%. ^{1}H NMR (300 MHz, DMSO-d_6): δ 8.49 (s, 1H), δ 8.04 (s, 1H), 7.64 (s, 1H), 5.13 (s, 1H), 5.00 (d, J = 13.8 Hz, 1H), 4.83 (m, 1H), 4.26 (m, 3H), 4.03 (m, 1H), 2.54 (s, 3H), 2.45 (s, 3H), 1.49 (s, 6H), 1.40 (s, 3H), 1.25 (s, 3H) ppm.

Intermediate 3: 3-bromopropylamine hydrobromide (5. g, 22.84 mmol) was dissolved in 75 mL of CH_2Cl_2 and 12.8 mL of triethylamine (4 eq) were added. The appearance of a white solid upon addiction of the amine indicated the formation of triethylammonium bromide. The mixture was left stirring for 30 min. Afterwards, the solution was cooled down to 0 ºC with an ice bath. Boc-anhydride (6g, 27.4 mmol) was dissolved in the minimum quantity of CH_2Cl_2 and dropwised to the amine solution. The mixture was stirred at room temperature overnight. Then, CH_2Cl_2 was removed under reduced pressure and the reaction crude washed with water, brine and 0.1 M HCl. A transparent oil (4.46 g) was isolated after drying with $MgSO_4$ and removing the solvent in the rotavapor. Yield: 82%. TLC: Hexane:EtOAc (8:2) (Rf: 0.6). ^{1}H NMR (300 MHz, $CDCl_3$): δ 4.69 (s, 1H), 3.45 (t, J = 6.5 Hz, 2H), 3.28 (t, J = 6.6 Hz, 2H), 2.12 – 2.01 (m, 2H), 1.46 (s, 9H) ppm.

Intermediate 4: 1.9 g of the protected flavin (2) (4.16 mmol), 1.25 g of Cs_2CO_3 (3.84 mmol) and 15 mL DMF were added into a 100 mL round bottom flask under N_2 atmosphere. The Boc-protected Br-propylamine (**3**) (2.98 g, 12.5 mmol) was dissolved in 10 mL of DMF and added drop by drop to the initial solution. The mixture was left stirring at room temperature overnight under N_2 atmosphere. The reaction mixture was extracted with CH_2Cl_2:LiCl (aq. 10%, 30 mL x 3) and dried with $MgSO_4$ to obtain a dark oil. 1 g of pure product was recovered after chromatographic column (SiO_2 gel for chromatography, 0.035-0.070 mm, 60 Å) in CH_2Cl_2:Acetone (85:15). Yield: 40%. TLC: EtOAc (Rf: 0.8). ^{1}H NMR (300 MHz, $CDCl_3$): δ 8.07 (s, 1H), 7.66 (s, 1H), 5.49 (s, 1H), 5.17 (d, J = 13.8 Hz, 1H), 5.01 (d, J = 10.7 Hz, 1H), 4.82 (d, J = 2.8 Hz, 1H), 4.27 (s, 3H), 4.21 (s, 2H), 4.10 – 4.02 (m, 1H), 3.15 (s, 2H), 2.56 (s, 3H), 2.47 (s, 3H), 1.94 (t, J = 6.3 Hz, 2H), 1.63 (s, 10H), 1.53 – 1.51 (m, 5H), 1.47 (s, 9H) ppm.

Rf-NH_2: 1g (1.6 mmol) of Intermediate 4 was dissolved in 80 mL of CH_2Cl_2. The mixture was cooled down over an ice bath for 30 min and the TFA (3 mL) was added drop by drop to the solution, which turned into a darker color. The mixture was left stirring at room temperature overnight. A small chromatographic column (SiO_2 gel for chromatography, 0.035-0.070 mm, 60 Å) was performed using 80:20 CH_2Cl_2:MeOH to isolate the desired product as a yellow powder. Yield: 93%. ^{1}H NMR (300 MHz, D2O): δ 8.07 (s, 1H), 7.98 (s, 1H), 5.22 – 5.05 (m, 1H), 4.44 (dd, J = 6.0, 3.5 Hz, 1H), 4.20 (t, J = 6.6 Hz, 2H), 3.90 – 3.80 (m, 3H), 3.74 – 3.67 (m, 1H), 3.07 (t, J = 7.3 Hz, 2H), 2.60 (s, 3H), 2.50 (s, 3H), 2.18 – 2.08 (m, 2H) ppm. ^{13}C NMR (75 MHz, D2O) δ 161.22, 157.10, 150.64, 148.45, 139.26, 134.91, 133.48, 131.86, 130.42, 116.67, 73.10, 72.36, 69.21, 62.57, 47.39, 38.89, 37.07, 25.19, 20.78, 18.62 ppm. ^{1}H NMR, ^{13}C NMR, COSY, HSQC and HMBC spectra are reported in the Supporting Information (Figures S1-S6).

Synthesis of AG-G

AG-G pathway involved two steps; (a) the alkoxylation of the C6 of the agarose with *rac*-glycidol and (b) the mild oxidation of the formed vicinal diols with $NaIO_4$ (see Supporting Information for details, Figure S7).[12]

Synthesis of AG-E

AG-E pathway involved one step: (a) the Williamson reaction of the agarose C6 hydroxyl with *rac*-epichlorohydrin, forming the desired epoxides (see Supporting Information, Figure S7).[18]

Flavin immobilization: on AG-E, in AG-G and in DEAE

AG-E: Approximately 50 mg of AG-E were prewashed three times by soaking and shaking the microbeads in phosphate buffer 0.1 M pH: 8 (0.5 mL x 3) (10 min). Then, **Rf-NH_2** (3 mM, 0.5 mL) was dissolved in the same buffer and sequentially loaded on the AG beads. The suspension was incubated in the dark for 6 h at 298 K and rotary mixed at 40 rpm. Afterwards, the supernatant was filtered and the beads were washed (0.5 mL x 3) with phosphate buffer 0.1 M (pH 8). Release of non-immobilized riboflavin at each washing was determined by UV-Vis spectroscopy (absorbance at 448 nm). Glycine (0.5 mL,1 M) in 0.1 M phosphate buffer (pH 8) was added and the suspension was incubated for 2 h at room temperature. The last step was needed to inactivate the remaining unreacted epoxy groups. The hydrogel was spun washed (0.5 mL x 3) with phosphate buffer 0.1 M (pH 8) and stored at 4ºC or directly used.

AG-G: Approximately 50 mg of AG-G were prewashed three times by soaking and shaking for 10 min (0.5 mL x 3) the microbeads in carbonate-bicarbonate buffer (0.1 M, pH 10). Then, **Rf-NH_2** (0.15-3 mM, 0.5 mL) was dissolved in the same buffer and sequentially loaded on the AG beads. The suspension was incubated in dark conditions for 6 h at 25 ºC and rotary mixed at 40 rpm. Afterwards, the supernatant was filtered and the hydrogel was washed with buffer (0.5 mL x 3). Release of non-immobilized riboflavin at each washing was determined by UV-Vis spectroscopy (absorbance at 428 nm). $NaBH_4$ (0.5 mL, 1 mg/mL) in carbonate-bicarbonate buffer (0.1 M, pH 10) was added and the suspension was incubated for 1 h at room temperature. The last step is needed to reduce the imine bond as well as the remaining unreacted aldehyde groups. The hydrogel was spun washed with the previous buffer (0.5 mL x 3) and stored at 4ºC or directly used.

AG-DEAE: **FMN**@AG-DEAE were prepared as described in our previous work.[8] Approximately 50 mg of AG-DEAE were prewashed three times by soaking and shaking the microbeads for 10 min (0.5 mL x 3) in Tris buffer (10 mM, pH 7.6). Then, **FMN** (0.15-1 mM, 0.5 mL) was dissolved in the same buffer and sequentially loaded on the AG beads. The suspension was incubated in dark conditions for 30 min at 25 ºC and rotary mixed at 40 rpm. Afterwards, the supernatant was filtered and the hydrogel was washed with buffer (0.5 mL x 3). Release of non-immobilized **FMN** at each washing was determined by UV-Vis spectroscopy (absorbance at 445 nm).

Assay for NADH oxidation

All catalytic experiments were carried out in air at 298 K. Light irradiation experiments were performed employing a LED light source (λ_{exc}= 456 nm, 0.1 mW·cm^{-2}). NADH consumption with and without light irradiation was determined for both free and immobilized flavins. NADH absorption was measured in a microplate reader BioTek Synergy H1. The UV detector wavelength was set at 340 nm. Total run time was 100 min or 24 h, with and without light irradiation respectively. Stock solutions/suspensions of flavin were prepared as described in Table S1 (see Supporting Information).

NADH/NAD^+ conversion experiments: 60 µL of 1mM NADH stock solution in distilled H_2O were added into the wells of a plate to reach a final concentration of 400 µM in all the experiments. Afterwards, a solution or suspension of free and immobilized flavins, respectively, were placed to start the reaction. The added volume of flavin for every experiment is depicted in Table S1 (see Supporting Information). The final concentration of flavin varies from 100 µM to 40 µM depending on the NADH/flavin ratio (4:1 or 10:1, respectively). Milli-Q H_2O was used to complete 150 µL total volume in all the well-plates. All experiments were performed in triplicates and all data are expressed as the mean ± standard deviation. Control experiments included NADH solutions (100 µM) and flavin solution/suspension without NADH (Rf, **FMN**@AG-DEAD and **Rf-NH_2**@AG-G) (100 µM and 40 µM) with and without light irradiation. The absorption values of flavins at 340 nm was subtracted in all experiments in order to obtain a more accurate comparison of the different systems.

Enzyme production

Alcohol dehydrogenase from *Bacillus stearothermophilus* (BsADH) was overexpressed in Escherichia coli BL21 cells. A total of 1 mL of an overnight culture of *E. coli* transformed with the pET28b-bsadh plasmid was inoculated in a 50 mL of Luria-Bertani (LB) broth containing kanamycin (final concentration of 30 μg x mL^{-1}). The culture was incubated at 37°C at 250 rpm until the $OD_{600\ nm}$ reached 0.6. At that point, the culture was induced with 1 mM of isopropyl β-d-1-thiogalactorpyranoside (IPTG). Cells were grown at 37°C for 3 h and then harvested by centrifugation at 10000 g during 30 min at 4°C.
The recombinantly expressed BsADH enzyme was purified by affinity as follows: the resulting pellet was resuspended in 5 mL of 50 mM sodium phosphate buffer solution (pH 8) with 10 mM imidazole. Cells were broken by sonication at an amplitude of 40% with alternating cycles of 3s-on / 5s-off during 15 min at 4°C (Sonopuls HD 4100, Bandelin). The cell lysate was centrifuged at 10000 g for 30 min at 4°C. The supernatant containing the enzyme was collected and passed through a cobalt-activated agarose resin equilibrated with a binding buffer (the same buffer used to resuspend the pellet). The column was incubated for 1 h at 4°C to promote the protein binding to the column. Afterward, the binding buffer was removed from the column by gravity and 5 mL of elution buffer (50 mM sodium phosphate buffer solution at pH 8 with 500 mM imidazole) was added to the column and incubated for 30 minutes at 4°C. The eluted protein was obtained by collecting the elution buffer by gravity from the column. Finally, the eluted protein was gel-filtered by using PD-10 columns (GE healthcare) to remove the imidazole and exchange the enzyme buffer for a sodium phosphate buffer with concentration and pH according to the experiment. SDS-PAGE and Bradford assays[2] were carried out after every protein production to determine the purity and concentration of the enzyme.

ADH activity assay

A reaction mixture containing NAD^+ (1 mM), 1,5-pentanodiol (10 mM) in sodium phosphate buffer (50 mM, pH 8) was incubated with 10 μl immobilized enzyme suspension (properly diluted) at 30ºC. The volume of the reaction mixture used was 200 μl and the increase in the absorbance at 340 nm due to the NADH formation was recorded for 30 minutes in stirring. To measure the activity of BsADH in solution, the volume of enzymatic solution (properly diluted) used was 5 μl. To measure the BsADH activity immobilized on AG-DEAE, the concentration of sodium phosphate buffer was 10 mM to avoid the enzyme lixiviation. Enzyme activities were spectrophotometrically measured in transparent 96-well microplates, employing a Microplate reader Epoch 2, BioTek with the software Gen5. One unit of activity is defined as the amount of enzyme needed to reduce 1 μmol of NAD^+ to NADH per minute.

ADH co-immobilization with FMN in AG-DEAE

First, 100 mg of diethylaminoethyl agarose microbeads (AG-DEAE) were prewashed (3 x 1mL) in Tris-HCl buffer (10 mM, pH 8); afterwards, the microbeads were incubated 30 minutes with 1mL of **FMN** solution with different concentrations (0.15-1 mM) according to the experiments. The incubation was made in a rotary mixer and room temperature; the supernatant was then removed by filtration through a minispin column after centrifugation. The **FMN**@AG-DEAE beads were then incubated with 1 mL of BsADH solution (0.1 mg/ml) in sodium phosphate buffer (10 mM, pH 7) for 30 minutes in a rotary mixer and room temperature. The supernatant was removed by filtration through a minispin column after centrifugation and the BsADH/**FMN**@AG-DEAE were washed (3 x 1mL) in sodium phosphate buffer (10 mM, pH 7). All the recovered supernatants were analysed by UV-Vis to calculate the flavin immobilization yield. The immobilization yield of BsADH was monitored by measuring the remaining ADH in the supernatant after the second filtration by the Bradford assay.[19]

ADH co-immobilization with Rf-NH_2 in AG-G

Initially, 100 mg of glyoxyl agarose microbeads (AG-G) were incubated 6 hours with 1 mL of solution containing **Rf-NH_2** (0.15 mM) in bicarbonate buffer (100 mM, pH 10). The incubation was made in a rotary mixer and room temperature; after that, the supernatant was removed by filtration through a minispin column after centrifugation. The recovered supernatant was analysed by UV-Vis in order to calculate the flavin immobilization yield. Subsequently, the **Rf-NH_2**@AG-G beads were incubated with 1 mL of BsADH solution (0.1 mg/ml) in bicarbonate buffer (100 mM, pH 10) for 30 minutes in a rotary mixer at 4ºC. Then, sodium borohydride ($NaBH_4$) was added to the mix (final concentration = 1 mg/ml). The incubation with $NaBH_4$ was 30-minute long and made in a rotary mixer at 4ºC. The supernatant was removed by filtration through a minispin column after centrifugation and the **Rf-NH_2**@AG-G beads were washed (3 x 1mL) in sodium phosphate buffer (50 mM, pH 8). The immobilization yield of BsADH was monitored by measuring the remaining ADH in the supernatant after filtration by the Bradford assay.[19]

Oxidation of 1,5-pentanodiol

30-42 μg of the heterogeneous (organo)biocatalysts were placed inside a capped plastic tube (2 mL) containing a reaction mixture (200 μl) of 10 mM 1,5-pentanodiol, 2 mM of NAD^+, 50 U of catalase from bovine liver (CAT) in 10 mM sodium phosphate buffer at pH 7. The reactions were incubated at 30ºC and in stirring at 250 rpm for the reaction time according to the experiments. In all reactions, 8.6 mU of BsADH activity were added to the reaction mix. In the case of the negative-control samples the AGM with the BsADH enzyme were not used. For those reactions that employed covalent co-immobilization, 50 mM sodium phosphate buffer was used. After the reaction time, the solution containing the reaction mix and the AGM was placed in a minispin column, and the supernatant was collected in a capped plastic tube (1.5 mL) after centrifugation.
In the case of the reuses, the immobilized (organo)biocatalysts were collected in the minispin column after centrifugation, then washed (3 x 1 mL) and finally stored at 4ºC till the following reaction. The preparation of the sample, the reaction mixes and the collection of the supernatant in the next reactions were the same as described before. The concentration of substrate and products in the supernatant were determined by gas chromatography analysis (GC).

GC-FID analysis

Prior to GC analysis, reaction samples were processed through a liquid – liquid extraction to extract the diol and its products (lactol and lactone) from the supernatants. The extraction is made with ethyl acetate as follows: 50 µl of sample's supernatant were mixed with 200 µl of ethyl acetate containing 2 mM eicosane as internal standard, then vortexed for 20 s and centrifuged 1 min at 1000 g. After extraction, the organic phase was placed in a capped plastic tube (1.5 mL) and 30-50 mg of anhydrous MgSO4 were added to dry the sample. Samples were injected in a Gas chromatograph. GC analyses were carried out in an Agilent 8890 GC system chromatograph using a J&W HP-5 GC column (30 m x 0.32 mm x 0.25 µm), He as the carrier gas and equipped with a flame ionization detector (FID). Injector at 280°C, FID at 300°C. The temperature program of the GC separation was: the initial temperature at 60°C, maintained 2 min, ramp to 160°C at a rate of 10°C min^{-1}, ramp 2 to 240°C at a rate of 20°C min^{-1} and finally maintained 4 min. [14]

Supporting Information

Additional references cited within the Supporting Information.[20-21]

Acknowledgements

M.J.M. has received funding from the EU Horizon 2020 Research and Innovation Programme under the Marie Sklodowska-Curie Actions grant no. 101024838. S.C.P. has received funding from the Agencia Estatal de Investigación through a predoctoral fellowship (PRE2020-093460). L.S. is grateful to the Diputación Foral de Gipuzkoa (RED 2021), and the Basque government (Eusko Jaurlaritza, grant PIBA_2021_1_0034). The authors thank the Spanish Multi-MetDrugs and Biocatalysis networks (RED2018-102471-T and RED2018-102403-T) for fruitful discussion. This work was performed under the Maria de Maeztu and Severo Ochoa Centers of Excellence Program run by the Spanish State Research Agency, grant no. MDM-2017-0720 (CIC biomaGUNE) and CEX2018-000867-S (DIPC). F.L-G and L.S thanks IKERBASQUE for sponsoring them.

Keywords: • Heterogeneous catalysis • Hybrid biomaterials • Flavins • Dehydrogenases • $NADH/NAD^+$

References

[1] Z. Guo, B. Liu, Q. Zhang, W. Deng, Y. Wang, Y. Yang, *Chem. Soc. Rev.* **2014**, *43*, 3480-3524.
[2] R. A. Sheldon, *ACS Sustain. Chem. Eng.* **2018**, *6*, 32-48.
[3] S. Wu, R. Snajdrova, J. C. Moore, K. Baldenius, U. T. Bornscheuer, *Angew. Chem. Int. Ed.* **2021**, *60*, 88-119.
[4] J. Santiago-Arcos, S. Velasco-Lozano, E. Diamanti, A. L. Cortajarena, F. López-Gallego, *Front. Catal.* **2021**, *1*, 9.
[5] X. Chen, Y. Cui, J. Feng, Y. Wang, X. Liu, Q. Wu, D. Zhu, Y. Ma, *Adv. Synth. Catal.* **2019**, *361*, 2497-2504.
[6] J. B. Jones, K. E. Taylor, *J. Chem. Soc., Chem. Commun.* **1973**, 205-206.
[7] M. Rauch, S. Schmidt, I. W. C. E. Arends, K. Oppelt, S. Kara, F. Hollmann, *Green Chem.* **2017**, *19*, 376-379.
[8] S. Velasco-Lozano, S. A.-d. Castro, C. Sanchez-Cano, A. I. Benítez-Mateos, F. López-Gallego, L. Salassa, *Chem. Sci.* **2022**, *13*, 59-67.
[9] S. Alonso-de Castro, A. L. Cortajarena, F. López-Gallego, L. Salassa, *Angew. Chem. Int. Ed.* **2018**, *57*, 3143-3147.
[10] J. Rocha-Martín, D. Vega, J. M. Bolivar, C. A. Godoy, A. Hidalgo, J. Berenguer, J. M. Guisán, F. López-Gallego, *BMC Biotechnol.* **2011**, *11*, 101-101.
[11] J. Chen, Q. Ma, M. Li, W. Wu, L. Huang, L. Liu, Y. Fang, S. Dong, *Nanoscale* **2020**, *12*, 23578-23585.
[12] C. Mateo, J. M. Palomo, M. Fuentes, L. Betancor, V. Grazu, F. López-Gallego, B. C. C. Pessela, A. Hidalgo, G. Fernández-Lorente, R. Fernández-Lafuente, J. M. Guisán, *Enzyme Microb. Technol.* **2006**, *39*, 274-280.
[13] J. Gurruchaga-Pereda, V. Martínez-Martínez, E. Rezabal, X. Lopez, C. Garino, F. Mancin, A. L. Cortajarena, L. Salassa, *ACS Catal.* **2020**, *10*, 187-196.
[14] S. Velasco-Lozano, J. Santiago-Arcos, M. Grazia Rubanu, F. López-Gallego, *ChemSusChem* **2022**, *15*, e202200397.
[15] J. Gurruchaga-Pereda, V. Martínez-Martínez, E. Formoso, O. Azpitarte, E. Rezabal, X. Lopez, A. L. Cortajarena, L. Salassa, *J. Phys. Chem. Lett.* **2021**, *12*, 4504-4508.
[16] V. Massey, *J. Biol. Chem.* **1994**, *269*, 22459-22462.
[17] L. F. Mazzei, J. Gurruchaga-Pereda, Á. Martínez, J. C. Martínez, L. Salassa, A. L. Cortajarena, *Chem. Commun.* **2023**, *59*, 4754-4757.
[18] C. Mateo, R. Torres, G. Fernández-Lorente, C. Ortiz, M. Fuentes, A. Hidalgo, F. López-Gallego, O. Abian, J. M. Palomo, L. Betancor, *Biomacromolecules* **2003**, *4*.
[19] M. M. Bradford, *Anal. Biochem.* **1976**, *72*, 248-254.
[20] A. Pines, M. G. Gibby, J. S. Waugh, *J. Chem. Phys*. **1973**, *59*, 569–590
[21] L. Mazzei, J. Gurruchaga-Pereda, A. Martínez, L. Salassa, J. Calvo Martínez, A. L. Cortajarena, *Chem. Commun.* **2023**, 59, 4754-4757